Please cite this article in press as: Bendezú and Martin, Cdc42 Explores the Cell Periphery for Mate Selection in Fission Yeast, Current Biology (2013), http://dx.doi.org/10.1016/j.cub.2012.10.042

Current Biology *23*, 1–6, January 7, 2013 ©2013 Elsevier Ltd All rights reserved http://dx.doi.org/10.1016/j.cub.2012.10.042

Report

# Cdc42 Explores the Cell Periphery for Mate Selection in Fission Yeast

**Felipe O. Bendezú[1] and Sophie G. Martin[1,*]**
[1]Department of Fundamental Microbiology, Faculty of Biology and Medicine, University of Lausanne, Biophore Building, 1015 Lausanne, Switzerland

## Summary

**How cells polarize in response to external cues is a fundamental biological problem. For mating, yeast cells orient growth toward the source of a pheromone gradient produced by cells of the opposite mating type [1, 2]. Polarized growth depends on the small GTPase Cdc42, a central eukaryotic polarity regulator that controls signaling, cytoskeleton polarization, and vesicle trafficking [3]. However, the mechanisms of polarity establishment and mate selection in complex cellular environments are poorly understood. Here we show that, in fission yeast, low-level pheromone signaling promotes a novel polarization state, where active Cdc42, its GEF Scd1, and scaffold Scd2 form colocalizing dynamic zones that sample the periphery of the cell. Two direct Cdc42 effectors—actin cables marked by myosin V Myo52 and the exocyst complex labeled by Sec6 and Sec8—also dynamically colocalize with active Cdc42. However, these cells do not grow due to a block in the exocytosis of cell wall synthases Bgs1 and Bgs4. High-level pheromone stabilizes active Cdc42 zones and promotes cell wall synthase exocytosis and polarized growth. However, in the absence of prior low-level pheromone signaling, exploration fails, and cells polarize growth at cell poles by default. Consequently, these cells show altered partner choice, mating preferentially with sister rather than nonsister cells. Thus, Cdc42 exploration serves to orient growth for partner selection. This process may also promote genetic diversification.**

## Results and Discussion

The rod-shaped fission yeast *S. pombe*, which proliferates asexually as a haploid through growth at cell poles, undergoes sexual differentiation in conditions of starvation. When starved of nitrogen in the presence of mating partners, cells arrest in G1 after one or two mitotic divisions, express pheromone and pheromone receptor, and polarize growth toward a partner (a process called shmooing) for cell fusion, meiosis, and formation of resistant spores [4]. Most fission yeast strains, including the *h90* lab strain, are homothallic, where after about 50% of cell divisions, one daughter cell switches between the two mating types, *h+* (P) and *h−* (M), thus producing mating-competent sister cells [5].

In mating conditions, after the last cell division, wild-type *h90* cells extended a short mating projection in the direction of a partner (Figure 1A see also Movie S1 available online). Although this often occurred near one cell pole, 5% of cells grew from cell sides (n = 699), indicating that the entire cell periphery is permissive for shmoo initiation. Shmoo growth, even when initiated from the cell tips, often differed from that of the long axis of the cell (Figure 1B), with shmoos forming orthogonally even from this location. Overall, mating pairs formed preferentially between nonsister cells (63%, n = 2,362 pairs). Because only about half of all sister pairs are predicted to be of opposite mating types, we then directly assessed the partner choices made by these compatible sisters. We visualized mating types by imaging the endogenous expression of the Map3 M factor receptor tagged with GFP, which is expressed in a cell-type-specific manner only in P cells (Figure S1A). This experiment showed comparable results to the previous one, with overall 61% of mating pairs formed between nonsister cells (n = 343 pairs). Remarkably, when considering in the same experiment only sister cells of opposite mating types, the first of the two sisters to engage in mating chose a neighboring nonsister cell as mate 53% of the time (n = 172 choices), despite the presence of a compatible sister as closest possible mate. In this and other experiments, change of partner was occasionally observed when the target partner became engaged (1% of mated cells, n = 699) (Figure S1B). These observations suggest fission yeast cells have an adaptable polarization mechanism for partner selection.

During mitotic growth, the conserved small GTPase Cdc42 breaks symmetry in spherical budding yeast cells [6, 7] and oscillates between poles in fission yeast [8]. We visualized active Cdc42 with an exogenous CRIB-GFP fusion that specifically binds GTP-bound Cdc42 [8, 9]. CRIB-GFP localized to shmoo tips, as expected. However, before shmoo formation, CRIB-GFP displayed a novel behavior: it localized dynamically to discrete zones around the cell periphery, appearing and disappearing at distinct locations, exploring over time a substantial part of the cell surface (Figure 1C and Movie S2). At any given time, this behavior occurred in a large fraction of cells (83%, n = 442) in both mating types (Figure S1F) and continued until a mating projection formed from a CRIB-GFP zone. Dynamic exploration could go on for many hours (at least up to 18 hr) when there was no close partner. The guanine nucleotide exchange factor (GEF) Scd1-3GFP and the scaffold protein Scd2-mCherry, which activate Cdc42 during mating [10], displayed similar behavior and colocalized extensively with CRIB (Figures 1D–1F and Movie S3): Scd1-3GFP colocalized with Scd2-mCherry, which itself colocalized with CRIB-GFP. We did not examine Cdc42 directly, because no functional Cdc42 fusion exists. Because Scd1-3GFP provided the strongest signal, we used it preferentially below. Thus, an active Cdc42 complex samples the cell periphery before specifying a site for mating projection formation.

High-resolution 4D imaging suggested that zones disassemble and assemble de novo rather than slide (Figure 1E), possibly through clustering of highly dynamic dots at the same location (Figure S1E). Dynamic dots were absent in shmooing cells, in which a single zone was present at the shmoo tip, suggesting clustering of all dots at this single site (Figure S1E). Zone formation was dependent on pheromone signaling, because zones (but not dots) were absent from starved heterothallic cells (cells of a single mating type that do not switch) (Figure S1E). Lower resolution but

*Correspondence: sophie.martin@unil.ch

Please cite this article in press as: Bendezú and Martin, Cdc42 Explores the Cell Periphery for Mate Selection in Fission Yeast, Current Biology (2013), http://dx.doi.org/10.1016/j.cub.2012.10.042



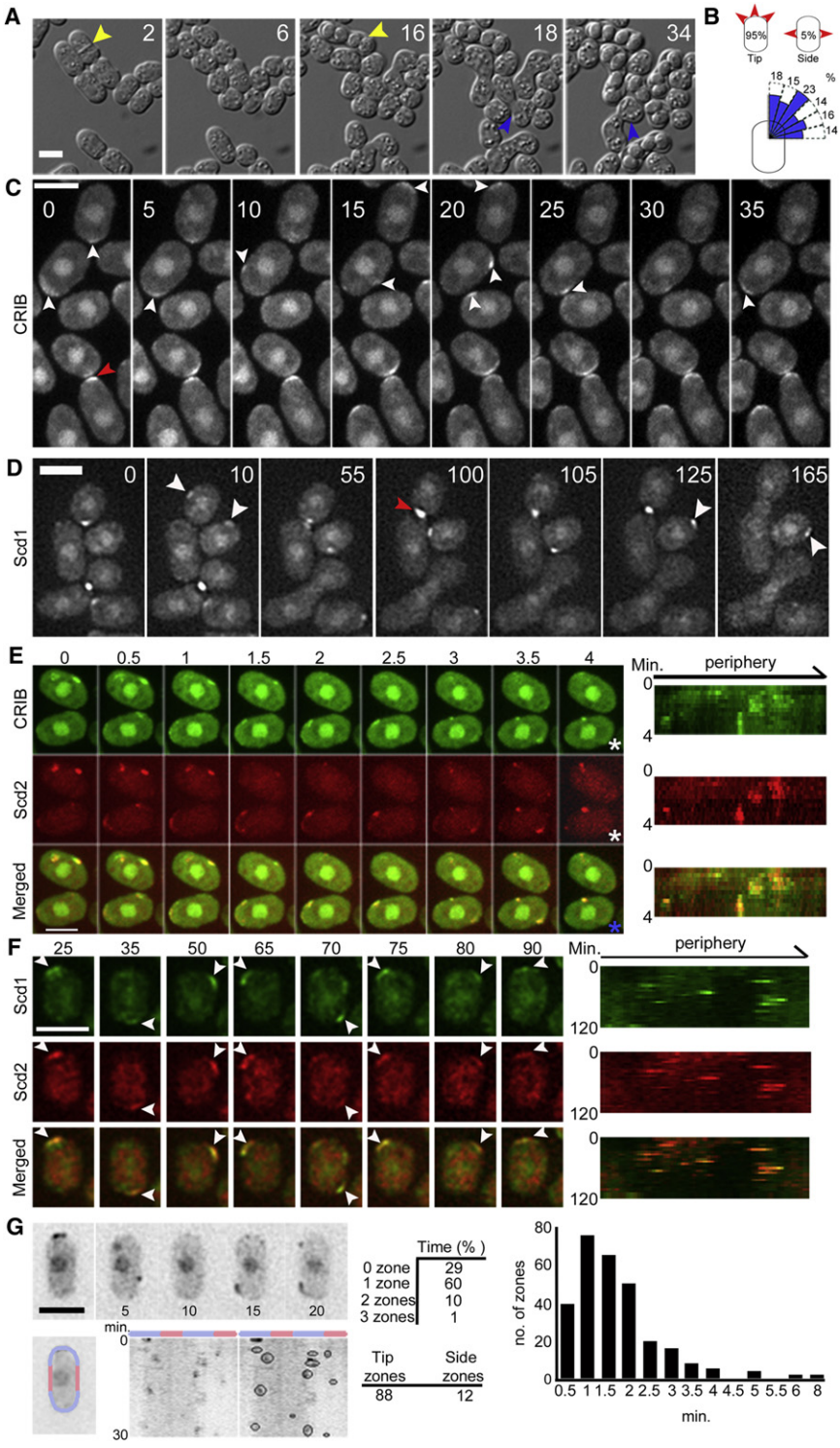


Figure 1. Cdc42 Zones Explore the Cell Periphery Prior to Mate Selection

(A) DIC images of *h90* cells mating on nitrogen-free agarose pads. Arrowheads highlight sister mating (yellow) and shmooing from cell side (blue).

(B) Quantification of shmoo position (top, n = 699) and direction (bottom, n = 200).

(C) Spinning disk confocal projections of CRIB-GFP.

(D) OAI (optical axis integration) imaging of Scd1-3GFP.

(E) Spinning disk confocal projections showing colocalization of Scd2-mCherry and CRIB-GFP with kymographs of the periphery of indicated cell (*, right).

(F) OAI imaging showing colocalization of Scd1-3GFP and Scd2-mCherry, with kymograph of the cell periphery (right).

(G) Quantification of OAI imaging of Scd1-3GFP. Left: selected inverted time points (top) and kymographs (bottom) with or without zones circled. Middle: percent of total time with indicated number and position of zones for 20 cells. Cell sides were defined as the cylindrical part of the cell and comprise an estimated 33% of total surface area. Right: distribution of zone dwell time for 20 cells.

All cells are *h90* wild-type cells. All time-lapse images were acquired every 5 min, except for (E) (30 s) and (G) (15 s). Arrowheads highlight dynamic (white) and shmoo tip (red) zones. Time is indicated in hr (A) or min (B–G). Scale bars represent 5 μm.

signal-preserving imaging experiments using real-time z sweep were used to quantify zone dynamics: single zones were observed 60% of the time, with two simultaneous zones occurring 10% of the time, usually as one zone appeared while another disappeared. These zones were highly variable in size (0.5 to 3 μm) and lifetime (average 1.5 min, Figure 1G) and formed around the entire cell periphery (88% in hemispherical polar regions versus 12% along cell sides). The sites of zone formation were likely influenced by the position of potential mating partners, because regions of partner proximity were often explored (Figure S1F). Positive and delayed negative feedback mechanisms are thought to govern Cdc42 polarization during vegetative polarization in budding and fission yeasts [6–8, 11]. Similar feedback mechanisms may operate during mating exploratory behavior to drive zone dynamics, with both types of feedbacks likely locally regulated by pheromone signaling.

We tested whether dynamic Cdc42 zones recruit downstream effectors. Cdc42 activates the formin For3, which assembles actin cables for myosin V-directed transport, and the exocyst, a complex that tethers incoming vesicles at the plasma membrane [12–14]. Together, these effectors promote the exocytosis of cell wall synthases [12] for cell wall remodeling and polarized growth. The myosin V Myo52, a marker for actin-cable origins, and the exocyst subunits Sec6 and Sec8 displayed dynamic localization around the cell periphery and colocalized with Scd1-3GFP and Scd2-mCherry, respectively (Figures 2A, 2B, and S2A). This suggests that each Cdc42 zone assembles actin cables and recruits the exocyst complex, poised for the polarized exocytosis of growth components. However, the cell wall synthases Bgs1 and Bgs4 did not colocalize with Scd2 at the cell periphery in exploring cells (Figure 2C, S2B,

Please cite this article in press as: Bendezú and Martin, Cdc42 Explores the Cell Periphery for Mate Selection in Fission Yeast, Current Biology (2013), http://dx.doi.org/10.1016/j.cub.2012.10.042



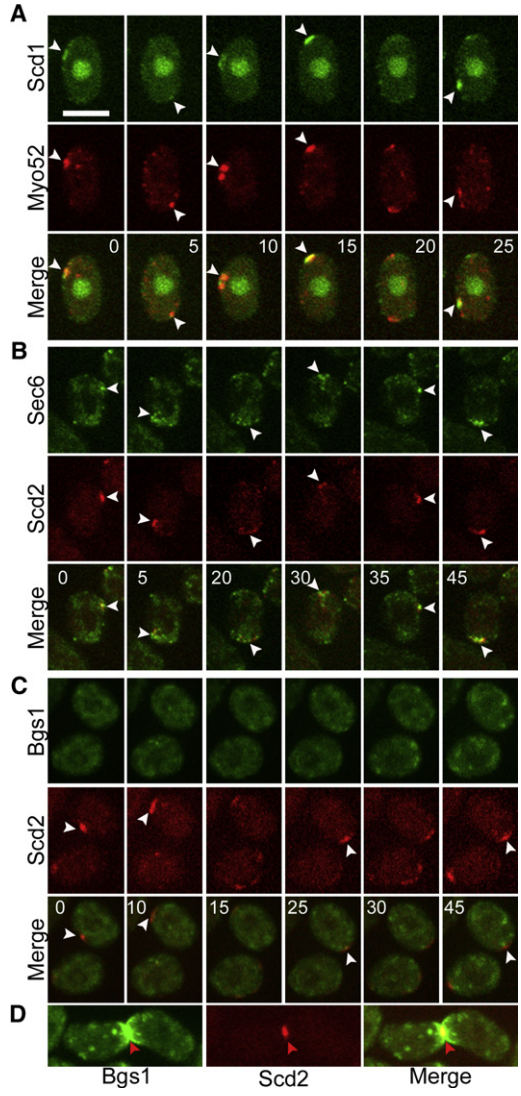


Figure 2. Exploratory Cdc42 Zones Recruit Polarization Effectors but Not Cell Wall Synthases

(A) Colocalization of Scd1-3GFP and Myo52-tdTomato.

(B) Colocalization of Scd2-mCherry and Sec6-GFP.

(C) Absence of colocalization of Bgs1-GFP with Scd2-mCherry exploratory zones.

(D) Colocalization of Bgs1-GFP and Scd2-mCherry at shmoo tips.

All cells are *h90* wild-type cells. All time-lapse images are spinning-disk confocal projections acquired every 5 min. Arrowheads highlight dynamic (white) and shmoo tip (red) zones. Time is indicated in min. Scale bars represent 5 μm.

and S2C). Instead, these enzymes localized to internal structures (Figures S2B, S2C, and S2E), suggesting that they are retained in endomembranes during Cdc42 dynamic behavior. Accordingly, cells did not grow appreciably even over long exploration periods (0.02 and 0.01 μm/hr length and width increase over 14 hr with corresponding estimated volume increase of 0.6 ± 0.6 $\mu m^3$/hr, n = 33). At later time points, by contrast, Bgs1 and Bgs4 localized strongly to mating projections, as shown previously [15] (Figures 2D and S2D), which grew at rates ranging between 0.37 and 1.03 μm/hr.

Thus, two distinct polarization stages occur successively during the mating process: in the first exploratory phase, zones of active Cdc42 form dynamically around the cell periphery but are not productive for growth because cell wall synthase exocytosis is blocked or not present at detectable levels at the cell cortex. In the second "committed" phase, a single reinforced Cdc42 zone promotes polarized growth through exocytosis of cell wall synthase. We note that even in the "committed" phase Cdc42 zone intensity fluctuates, with cells able to reenter the exploratory phase, especially if the target partner becomes engaged to another cell (Figures S1C and S1D).

We asked whether these two polarization stages could be triggered by the addition of synthetic pheromone. We used heterothallic M cells, which respond to exogenous P factor, in which the secreted Sxa2 protease that degrades P factor for desensitization [16, 17] was deleted. In absence of pheromones, Scd1 zones were not detected (Figure 3A). Low P factor levels (0.1 to 100 ng/ml) promoted the formation of dynamic Scd1 zones (Figure 3A and data not shown), but no growth (0.5 ± 0.4 $\mu m^3$/hr with 100 ng/ml P factor, compared to 0.8 ± 0.4 $\mu m^3$/hr without P factor, n = 20). As in mating mixtures, zones formed dynamically around the entire cell periphery with overall comparable frequency of zones on cell sides (Figure S3A). Duration of pheromone exposure had little influence on zone dynamics, which were observed as soon as 2 hr or as long as 14 hr after pheromone addition (Figure S3A). By contrast, high levels of P factor (from 500 ng/ml) induced Scd1 zones exclusively at cell poles (Figure 3A) and promoted polar growth (5.4 ± 4.0 $\mu m^3$/hr, n = 20), as shown previously [2]. Similar results were obtained using *pka1Δ* cells, which enter sexual differentiation in absence of starvation, indicating that exploratory behavior is a consequence of low-level pheromone signaling rather than starvation (Figure S3B). Thus, distinct pheromone levels produce polarization states akin to the two successive stages described above in mating mixtures.

The polar growth observed in high exogenous pheromone levels suggests that, in absence of the exploratory phase, cells choose cell poles by default, and that exploration may serve to overcome this default location. This default choice may be due to historical landmarks, some of which are dismantled during mating [18], or geometrical parameters. Remarkably, a small fraction of cells (0.3%, n = 6,800) successively exposed to low, then high levels of P factor formed T-shaped cells, indicating growth from cell sides (Figure 3B). Thus, even in artificial homogeneous pheromone conditions, prior low-level pheromone exposure can promote the positioning of a shmoo away from its default site at cell poles. During the normal mating process, increasing pheromone signaling may successively define the exploration and committed phases for shmoo orientation.

To further test the notion that distinct levels of pheromone signaling regulate polarization, we used mutants that promote constitutive high pheromone signaling. Heterotrimeric G protein-coupled pheromone receptors are downregulated by internalization, and truncation of the cytoplasmic tail of the M factor receptor Map3 (*map3$^{dn9}$*) prevents its internalization [19]. In *h90 map3$^{dn9}$-GFP* matings, mutant P cells, in which the mutant Map3$^{dn9}$ M factor receptor covers a large part of the cell membrane, did not exhibit Scd2 exploration around the entire cell periphery. Instead, they showed restricted Scd2 localization at cell poles, which retained dynamic fluctuations, and grew straight at their poles (Figures 3C, 3E, and Movie S4). In contrast, most M cells, which express the wild-type Mam2 P factor receptor, exhibited normal Scd2 exploration and shmooed toward a partner cell. In both cell types, pheromone

Please cite this article in press as: Bendezú and Martin, Cdc42 Explores the Cell Periphery for Mate Selection in Fission Yeast, Current Biology (2013), http://dx.doi.org/10.1016/j.cub.2012.10.042



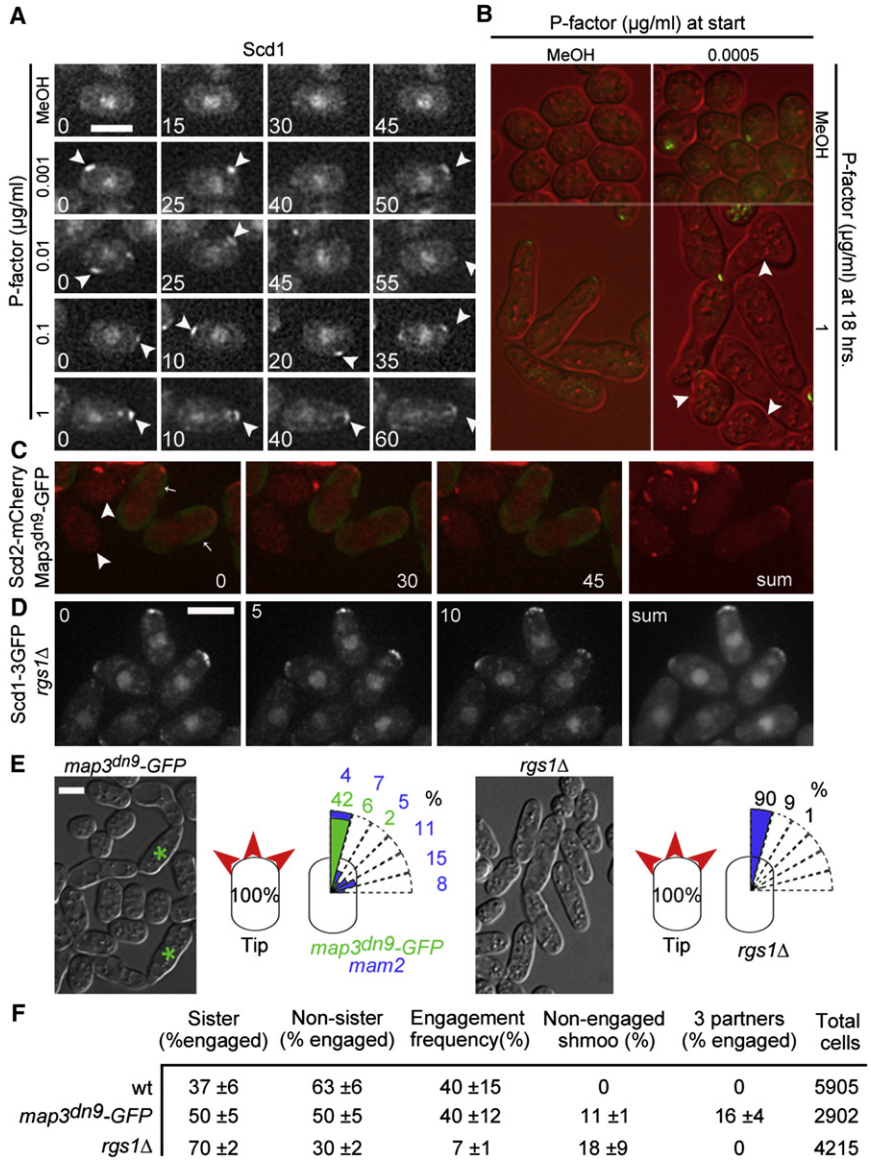


F

| | Sister (%engaged) | Non-sister (% engaged) | Engagement frequency(%) | Non-engaged shmoo (%) | 3 partners (% engaged) | Total cells |
|---|---|---|---|---|---|---|
| wt | 37 ±6 | 63 ±6 | 40 ±15 | 0 | 0 | 5905 |
| *map3dn9-GFP* | 50 ±5 | 50 ±5 | 40 ±12 | 11 ±1 | 16 ±4 | 2902 |
| *rgs1Δ* | 70 ±2 | 30 ±2 | 7 ±1 | 18 ±9 | 0 | 4215 |

Figure 3. Low-Level Pheromone Is Required for Cdc42 Zone Exploration, Shmoo Orientation, and Mate Choice

(A) Scd1-3GFP signals at indicated time after addition of increasing concentrations of P factor to *h- sxa2Δ* cells. Methanol solvent was used as control. Note Scd1 exploration (arrowheads) at concentration of P factor (0.001 to 0.1 μg/ml), insufficient to induce shmoo growth.

(B) DIC and Scd1-3GFP merged images of *h- sxa2Δ* cells treated first with methanol (left) or 0.5 ng/ml P factor (right) for 20 hr and then with methanol (top) or 1 μg/ml P factor (bottom) for another 18 hr. Low-to-high P factor treatment promotes shmoo growth from cell sides (arrowheads).

(C) Scd2-mCherry and GFP signals of *h90* cells expressing the truncated Map3$^{dn9}$-GFP receptor (arrows) or wild-type Mam2 receptor (arrowheads). Right panel shows maximum-intensity projection of the Scd2-mCherry signal over 2 hr (sum).

(D) Scd1-3GFP signals in *h90 rgs1Δ* cells. Sum = maximum-intensity projection over 1 hr.

(E) DIC image and quantification of shmoo position and direction of mating *h90 map3$^{dn9}$-GFP* and *h90 rgs1Δ* cells. Cells expressing Map3$^{dn9}$-GFP are marked with an asterisk. Compare to wild-type in Figures 1A and 1B.

(F) Quantification of partner choices made by *h90* WT and hypersignaling mutants.

Time is indicated in hours (A and B) or minutes (C and D). Scale bars represent 5 μm.

signaling is transmitted through the Gα subunit Gpa1 [20], which is negatively regulated by the regulator of G protein signaling protein Rgs1 [21, 22]. In *rgs1Δ* cells, in which Gpa1 is predicted to remain GTP-bound and active, Scd1-3GFP failed to explore the cell periphery and localized only at cell poles, resulting in straight mating projections (Figures 3D–3E). Thus, genetic mutations promoting high signaling levels, like addition of high levels of synthetic pheromone, block the exploratory phase and lead to default growth at cell poles.

Previous reports had shown that both *map3$^{dn9}$* and *rgs1Δ* mutations impair mating efficiency [19, 21, 22], but microscopic examination showed significant mating pair formation. Although mating type switching occurred at near wild-type rates in these mutant cells (Figure S3C), pairs between nonsister cells formed at a reduced frequency (Figure 3F), with *map3$^{dn9}$* pairs, where only one of the two partners expresses the mutant receptor and is deficient in exploration, showing intermediate values. Pairs of both *rgs1Δ* and *map3$^{dn9}$* often failed to fuse, suggesting signal downregulation is necessary for fusion. *Map3$^{dn9}$* cells are also often promiscuous, engaging with two partners at once (Figures 3E and 3F). Thus, lack of exploration and default choice of poles for growth correlate with a drop in mating between nonsister cells, a choice that may lead to a decrease in genetic exchange.

We propose that exploratory polarization serves to overcome cell pole polarity landmarks and permit orientation and mating partner choice, promoting in particular nonsister cell pairing (Figure 4). When exploration fails, cells polarize growth at cell poles by default and mate preferentially with their sister (Figure 3F). This may represent an ancient strategy, similar to the default strategy in *S. cerevisiae*, in which in the absence of orientation information, cells shmoo from bud site landmarks [23–26], thus failing to choose the highest pheromone-expressing mate [27, 28]. Because haploid *S. cerevisiae* cells bud axially, default mating may also favor sister cell mating, although this has, to our knowledge, not been tested.

Dynamic polarization strategies likely occur for other symmetry-breaking events. Mutant budding yeast cells lacking landmarks for bud site positioning (*rsr1Δ*) or lacking the molecular connection to pheromone sensing for shmoo orientation (*far1* mutants) exhibit considerable dynamics of polarization factors at the cell surface [11, 29, 30]. More constrained dynamic wandering of Cdc42 regulators has now also been described at the tip of wild-type *S. cerevisiae* shmoos exposed to subsaturating levels of pheromone, as seen in the accompanying manuscript by Dyer et al. in this issue of *Current Biology* [31]. Ras also dynamically localizes at random cell surface locations in *Dictyostelium* in absence of chemoattractants

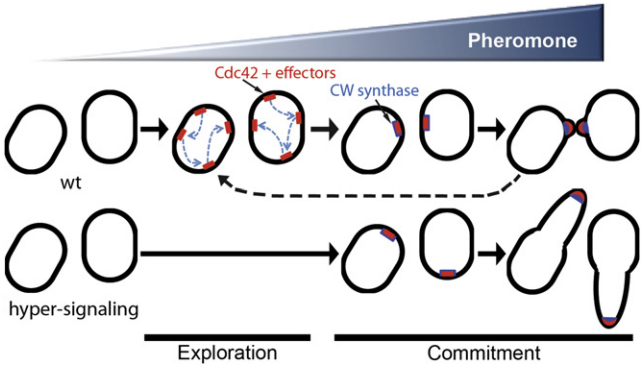


Figure 4. Schematic Model of Cdc42 Exploratory Polarization Behavior for Mate Selection

Low levels of pheromone stimulate dynamic exploration of cell periphery by active Cdc42 zones, which recruit polarization effectors. Upon mate choice, cell wall synthases are recruited, and cells shmoo toward a partner. If the mate cannot be engaged, cells are capable of reentering exploration phase (dashed line). Hypersignaling mutants or high levels of pheromone bypass normal exploration, and active Cdc42 localizes and promotes growth at cell tips by default.

[32], allowing the cell to migrate randomly to explore its environment. Despite the predicted high associated costs, exploration may represent a fundamental self-organizing mechanism for accurate and flexible gradient sensing.

### Experimental Procedures

Fission yeast strains used in this study are listed in Table S1. Standard genetic techniques were used. Mating assays and pheromone exposure experiments were performed on MSL medium lacking nitrogen, except for the *pka1Δ* experiment, which was done on MSL medium with nitrogen. Detailed descriptions of mating conditions, microscopy and image analysis, synthetic pheromone treatment, and mating-partner choice analysis are provided in the Supplemental Experimental Procedures.

### Supplemental Information

Supplemental Information includes three figures, one table, Supplemental Experimental Procedures, and four movies and can be found with this article online at http://dx.doi.org/10.1016/j.cub.2012.10.042.

### Acknowledgments

We would like to thank Masayuki Yamamoto and the Japanese National BioResource Project for strains and reagents; Niko Geldner, Richard Benton, and members of the lab for discussion and comments on the manuscript; and Daniel Lew for exchange of information before publication. F.O.B. was supported by a National Science Foundation postdoctoral fellowship (0852905). This work was supported by a Swiss National Science Foundation (SNF) Professorship grant (PP00A–114936) and a SNF Research grant (31003A_138177). Research in S.G.M.'s lab is also supported by a HFSP Career Development Award (CDA0016/2008) and a European Research Council Starting Grant (260493).

Received: August 9, 2012
Revised: October 9, 2012
Accepted: October 24, 2012
Published: November 29, 2012

### References

1. Segall, J.E. (1993). Polarization of yeast cells in spatial gradients of alpha mating factor. Proc. Natl. Acad. Sci. USA *90*, 8332–8336.
2. Imai, Y., and Yamamoto, M. (1994). The fission yeast mating pheromone P-factor: its molecular structure, gene structure, and ability to induce gene expression and G1 arrest in the mating partner. Genes Dev. *8*, 328–338.
3. Etienne-Manneville, S. (2004). Cdc42—the centre of polarity. J. Cell Sci. *117*, 1291–1300.
4. Davey, J. (1998). Fusion of a fission yeast. Yeast *14*, 1529–1566.
5. Klar, A.J. (2007). Lessons learned from studies of fission yeast mating-type switching and silencing. Annu. Rev. Genet. *41*, 213–236.
6. Johnson, J.M., Jin, M., and Lew, D.J. (2011). Symmetry breaking and the establishment of cell polarity in budding yeast. Curr. Opin. Genet. Dev. *21*, 740–746.
7. Slaughter, B.D., Smith, S.E., and Li, R. (2009). Symmetry breaking in the life cycle of the budding yeast. Cold Spring Harb. Perspect. Biol. *1*, a003384.
8. Das, M., Drake, T., Wiley, D.J., Buchwald, P., Vavylonis, D., and Verde, F. (2012). Oscillatory dynamics of Cdc42 GTPase in the control of polarized growth. Science *337*, 239–243.
9. Tatebe, H., Nakano, K., Maximo, R., and Shiozaki, K. (2008). Pom1 DYRK regulates localization of the Rga4 GAP to ensure bipolar activation of Cdc42 in fission yeast. Curr. Biol. *18*, 322–330.
10. Chang, E.C., Barr, M., Wang, Y., Jung, V., Xu, H.P., and Wigler, M.H. (1994). Cooperative interaction of *S. pombe* proteins required for mating and morphogenesis. Cell *79*, 131–141.
11. Howell, A.S., Jin, M., Wu, C.F., Zyla, T.R., Elston, T.C., and Lew, D.J. (2012). Negative feedback enhances robustness in the yeast polarity establishment circuit. Cell *149*, 322–333.
12. Bendezú, F.O., and Martin, S.G. (2011). Actin cables and the exocyst form two independent morphogenesis pathways in the fission yeast. Mol. Biol. Cell *22*, 44–53.
13. Estravís, M., Rincón, S.A., Santos, B., and Pérez, P. (2011). Cdc42 regulates multiple membrane traffic events in fission yeast. Traffic *12*, 1744–1758.
14. Martin, S.G., Rincón, S.A., Basu, R., Pérez, P., and Chang, F. (2007). Regulation of the formin for3p by cdc42p and bud6p. Mol. Biol. Cell *18*, 4155–4167.
15. Cortés, J.C., Carnero, E., Ishiguro, J., Sánchez, Y., Durán, A., and Ribas, J.C. (2005). The novel fission yeast (1,3)beta-D-glucan synthase catalytic subunit Bgs4p is essential during both cytokinesis and polarized growth. J. Cell Sci. *118*, 157–174.
16. Imai, Y., and Yamamoto, M. (1992). *Schizosaccharomyces pombe* sxa1+ and sxa2+ encode putative proteases involved in the mating response. Mol. Cell. Biol. *12*, 1827–1834.
17. Ladds, G., and Davey, J. (2000). Sxa2 is a serine carboxypeptidase that degrades extracellular P-factor in the fission yeast Schizosaccharomyces pombe. Mol. Microbiol. *36*, 377–390.
18. Niccoli, T., and Nurse, P. (2002). Different mechanisms of cell polarisation in vegetative and shmooing growth in fission yeast. J. Cell Sci. *115*, 1651–1662.
19. Hirota, K., Tanaka, K., Watanabe, Y., and Yamamoto, M. (2001). Functional analysis of the C-terminal cytoplasmic region of the M-factor receptor in fission yeast. Genes Cells *6*, 201–214.
20. Obara, T., Nakafuku, M., Yamamoto, M., and Kaziro, Y. (1991). Isolation and characterization of a gene encoding a G-protein alpha subunit from *Schizosaccharomyces pombe*: involvement in mating and sporulation pathways. Proc. Natl. Acad. Sci. USA *88*, 5877–5881.
21. Watson, P., Davis, K., Didmon, M., Broad, P., and Davey, J. (1999). An RGS protein regulates the pheromone response in the fission yeast *Schizosaccharomyces pombe*. Mol. Microbiol. *33*, 623–634.
22. Pereira, P.S., and Jones, N.C. (2001). The RGS domain-containing fission yeast protein, Rgs1p, regulates pheromone signalling and is required for mating. Genes Cells *6*, 789–802.
23. Butty, A.C., Pryciak, P.M., Huang, L.S., Herskowitz, I., and Peter, M. (1998). The role of Far1p in linking the heterotrimeric G protein to polarity establishment proteins during yeast mating. Science *282*, 1511–1516.
24. Nern, A., and Arkowitz, R.A. (1998). A GTP-exchange factor required for cell orientation. Nature *391*, 195–198.
25. Nern, A., and Arkowitz, R.A. (1999). A Cdc24p-Far1p-Gbetagamma protein complex required for yeast orientation during mating. J. Cell Biol. *144*, 1187–1202.
26. Valtz, N., Peter, M., and Herskowitz, I. (1995). FAR1 is required for oriented polarization of yeast cells in response to mating pheromones. J. Cell Biol. *131*, 863–873.
27. Jackson, C.L., and Hartwell, L.H. (1990). Courtship in *S. cerevisiae*: both cell types choose mating partners by responding to the strongest pheromone signal. Cell *63*, 1039–1051.

28. Dorer, R., Pryciak, P.M., and Hartwell, L.H. (1995). Saccharomyces cerevisiae cells execute a default pathway to select a mate in the absence of pheromone gradients. J. Cell Biol. *131*, 845–861.
29. Nern, A., and Arkowitz, R.A. (2000). G proteins mediate changes in cell shape by stabilizing the axis of polarity. Mol. Cell *5*, 853–864.
30. Ozbudak, E.M., Becskei, A., and van Oudenaarden, A. (2005). A system of counteracting feedback loops regulates Cdc42p activity during spontaneous cell polarization. Dev. Cell *9*, 565–571.
31. Dyer, J.M., Savage, N.S., Jin, M., Zyla, T.R., Elston, T.C., and Lew, D.J. (2012). Tracking shallow chemical gradients by actin-driven wandering of the polarization site. Curr. Biol. Published online November 29, 2012. http://dx.doi.org/10.1016/j.cub.2012.11.014.
32. Sasaki, A.T., Janetopoulos, C., Lee, S., Charest, P.G., Takeda, K., Sundheimer, L.W., Meili, R., Devreotes, P.N., and Firtel, R.A. (2007). G protein-independent Ras/PI3K/F-actin circuit regulates basic cell motility. J. Cell Biol. *178*, 185–191.

**Current Biology, Volume *23***
**Supplemental Information**

# Cdc42 Explores the Cell Periphery for Mate Selection in Fission Yeast

**Felipe O. Bendezú and Sophie G. Martin**

# Figure S1

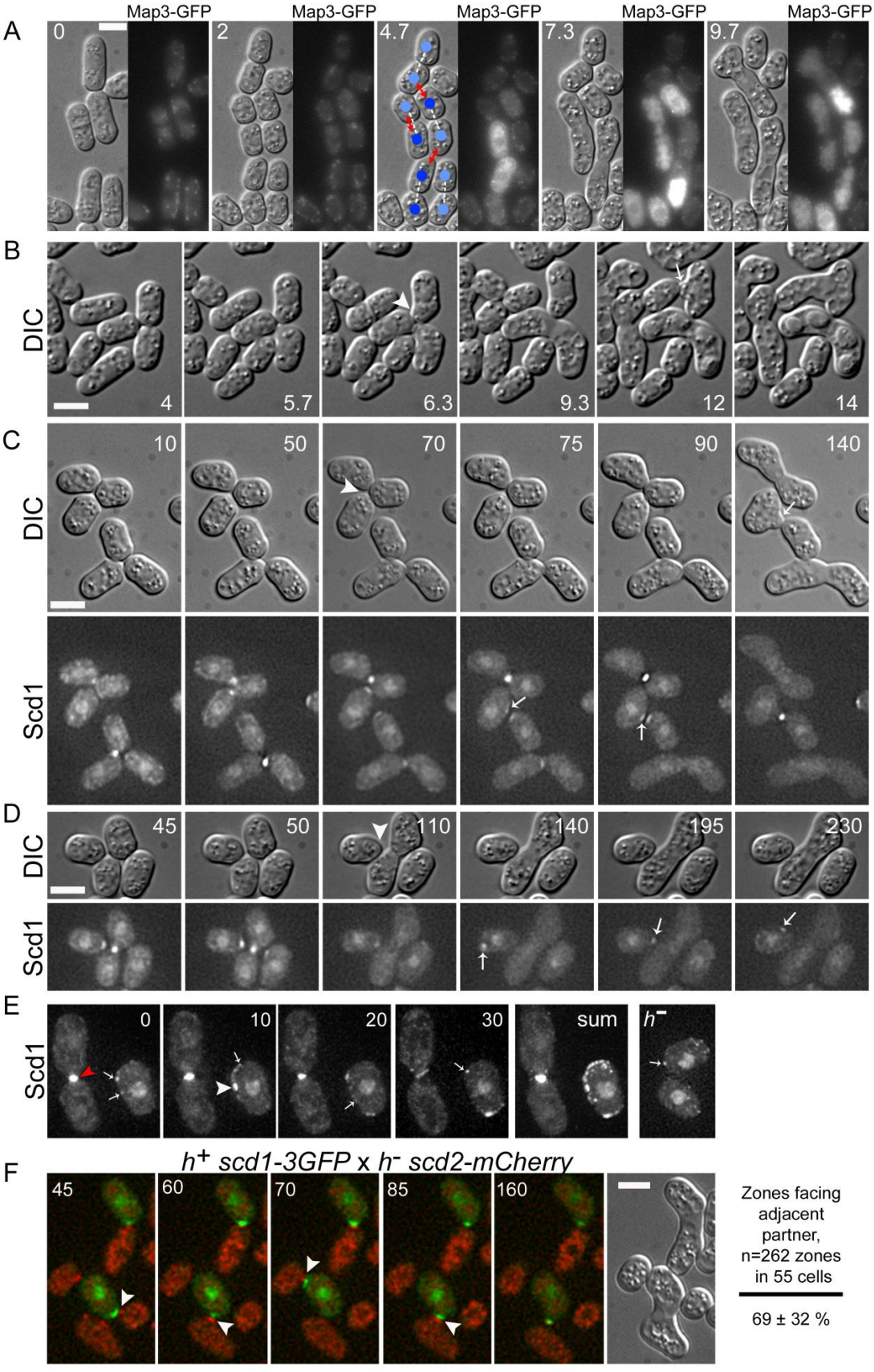
A
Map3-GFP
Map3-GFP
Map3-GFP
Map3-GFP
Map3-GFP
0
2
4.7
7.3
9.7
B
DIC
4
5.7
6.3
9.3
12
14
C
DIC
10
50
70
75
90
140
Scd1
D
DIC
45
50
110
140
195
230
Scd1
E
Scd1
0
10
20
30
sum
h⁻
F
h+ scd1-3GFP x h- scd2-mCherry
45
60
70
85
160
Zones facing adjacent partner, n=262 zones in 55 cells
69 ± 32 %

**Figure S1 (Related to Figure 1). Cells Committed to a Mate Can Re-enter Exploratory Phase and Engage with Another Mate; Detail of Dynamic Exploration**

(A) DIC and GFP fluorescence images of *h90* cells encoding a GFP fusion to the M factor receptor Map3. Note expression of Map3-GFP in *h*+ cells marked with dark blue circles at 4.7 hour time point. Light blue circles mark *h*- cells that do not expresses Map3-GFP. Dashed white lines indicate sister cells and red arrows indicate mated pairs. Time is in hours.

(B) DIC images of wildtype *h90* mating cells. The cell marked with an arrowhead shows a visible shmoo towards a prospective mate. When the prospective mate fuses with another cell the marked cell stops shmooing (arrowhead) and later engages with another mate (arrow). Time is in hours.

(C and D) DIC (upper) and GFP fluorescence (lower) images of wildtype *h90 scd1-3GFP* mating cells. Arrowheads show small shmoo growth that stops when prospective mate chooses another partner. Arrows show Scd1 re-enter exploratory phase. Time is in minutes.

(E) Deconvolved maximum-intensity projection of 3D DeltaVision imaging of Scd1-3GFP signals in *h90* mating cells showing zones (arrowhead) and dots (arrow) in an exploring cell and single zones (red arrowhead) with no dots in engaged cells. Dot signals are weak and not detected by either OAI imaging or spinning disk confocal microscopy shown in the other Figures. Time is in minutes. Sum = max-intensity projection of 25 images over 2 hours.

(F) OAI imaging of Scd1-3GFP and Scd2-mCherry signals in heterothallic *h*+ and *h*- mating cells, respectively. Arrowheads indicate coincident zones between cells of distinct mating type. DIC image shows fusion of cells following partner choice. The high percentage of zones localized adjacent to a possible partner (left) indicates zone location is influenced by partner position. Bars are 5 μm.

Figure S2

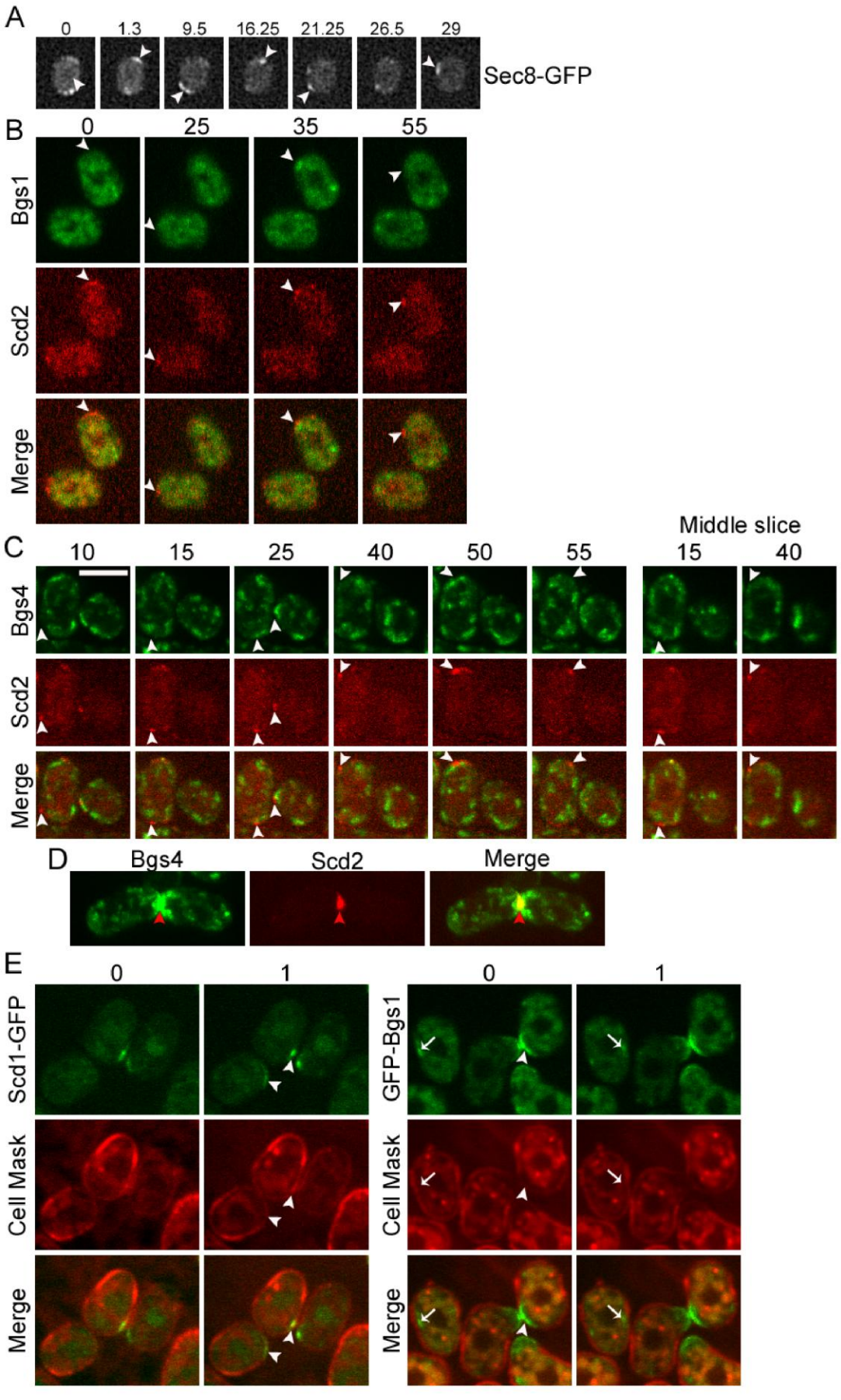
A
0
1.3
9.5
16.25
21.25
26.5
29
Sec8-GFP
B
0
25
35
55
Bgs1
Scd2
Merge
C
Middle slice
10
15
25
40
50
55
15
40
Bgs4
Scd2
Merge
D
Bgs4
Scd2
Merge
E
0
1
0
1
Scd1-GFP
GFP-Bgs1
Cell Mask
Cell Mask
Merge
Merge

**Figure S2 (Related to Figure 2). Exocyst Member Sec8 Explores Cell Periphery, but Cell Wall Synthases Bgs1 and Bgs4 Localize to Internal Structures during Cdc42 Exploration**
(A) OAI imaging showing exploration of Sec8-GFP.
(B) Middle optical z slice of the same cells shown in Figure 2C. Arrowheads indicate dynamic Scd2-mCherry zones.
(C) Absence of colocalization of Bgs4-GFP with Scd2-mCherry exploratory zones. Bgs4 localizes to distinct internal structures, which are often adjacent but not overlapping with Scd2 signal at the periphery. Right panels show the middle optical z slice only for indicated time points.
(D) Colocalization of Bgs4-GFP and Scd2-mCherry at shmoo tips (red arrowhead).
(E) Staining of *h90* exploring cells with Cell Mask, which labels the plasma membrane. This shows localization of Scd1 zones at the cell periphery (arrowheads). In contrast, Bgs1 label internal structures that do not colocalize with Cell Mask during exploration (arrow), while these enzymes localize at the cell periphery at shmoo tips (arrowheads).

# Figure S3

A

| P-factor (µg/ml) | 2 hours | | | 14 hours | | |
|---|---|---|---|---|---|---|
| | zones/cell | % side | n | zones/cell | % side | n |
| MeOH | 0 | 0 | 30 | 0 | 0 | 30 |
| 0.001 | 2.4 ±0.9 | 25 | 25 | nd | nd | nd |
| 0.01 | 3.6 ±1.5 | 13 | 26 | 2.0 ±0.8 | 23 | 36 |
| 0.1 | 3.5 ±1.4 | 4 | 33 | 2.4±0.8 | 8 | 26 |
| 1 | 1.3 ±0.5 | 0 | 32 | 1.3 ±0.5 | 0 | 26 |

B

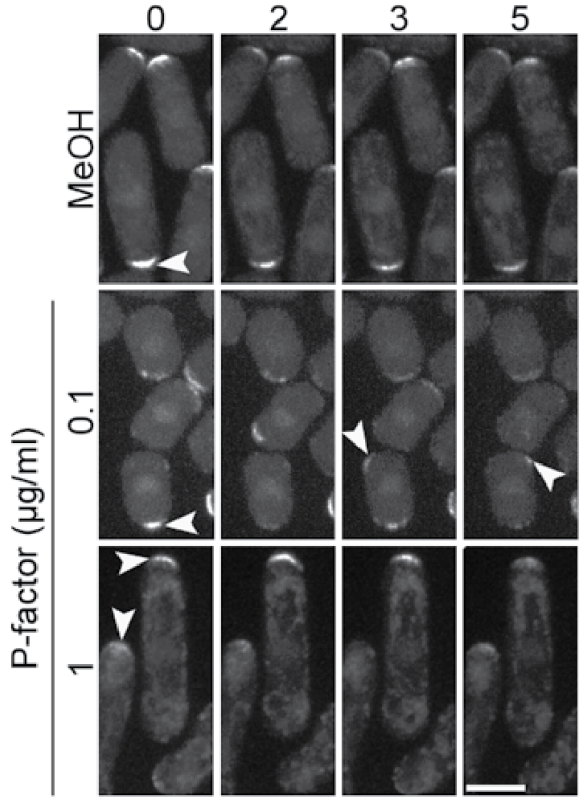


C

| | % Compatible sisters | n |
|---|---|---|
| *map3-GFP* | 46 | 131 |
| *map3$^{dn9}$-GFP* | 40 | 134 |
| *map3-GFP rgs1Δ* | 42 | 126 |

**Figure S3 (Related to Figure 3). Scd1-3GFP Zone Dynamics Quantification after Short and Prolonged Exposure to P Factor, Exploratory Polarization in *pka1*Δ Cells, and Mating-Type Switching Rates in Hypersignaling Mutants**

(A) Quantification of Scd1-3GFP zones per cell of *h- sxa2*Δ cells treated with methanol (MeOH) solvent control or increasing concentration of P-factor. Cells were grown in MSL-N for 4 hours before placement onto MSL-N agarose pads and incubated at 25$^{o}$C for 2 or 14 hours before imaging. Cells were imaged by OAI microscopy every 5 minutes for 1 hour. % side indicates the percent of zones present along the cell sides. Sides were defined as the cylindrical part of the cell, and comprise an estimated 33% of total surface area.

(B) Scd1-3GFP signals in *h- sxa2*Δ *pka1*Δ cells imaged on MSL media containing nitrogen and either P-factor or solvent methanol. We note cells treated with methanol were actively growing and dividing, indicating presence of sufficient nutrient for growth, whereas the majority of cells treated with P-factor had either arrested growth (0.1μg/ml) as judged by smaller cell size or were actively shmooing (1μg/ml). Arrowheads show zones of Scd1. Bar is 5 μm.

(C) Homothallic *h90* cells switch mating types in a pattern such that half the cells in a population are born with a compatible sister and the other half are born with a sister of the same mating type. The percent of cell pairs born with compatible sisters in wt *h90*, *h90 map3$^{dn9}$-GFP* and *h90 rgs1*Δ was determined by imaging the mating-type specific expression of the pheromone receptor Map3-GFP or the truncated Map3$^{dn9}$-GFP fusions.

**Table S1. Strains Used in This Study**

| | | |
|---|---|---|
| YSM1623 | *h90 bgs1::ura4+Pbgs1-GFP-bgs1-leu1+ leu1-32 ura4-D18* | This work |
| YSM2038 | *h90 sec8-GFP-ura4+* | This work |
| YSM2039 | *h+ scd1-3GFP-kanMX* | This work |
| YSM2040 | *h90 scd1-3GFP-kanMX* | This work |
| YSM2041 | *h90 scd1-3GFP-kanMX scd2-mCherry-natMX* | This work |
| YSM2042 | *h- scd2-mCherry-natMX* | This work |
| YSM2043 | *h90 scd1-3GFP-kanMX myo52-dtTomato-natMX* | This work |
| YSM2044 | *h- sxa2::kanMX scd1-3GFP-kanMX* | This work |
| YSM2045 | *h90 map3::ura4+ Pmap3-map3$^{dn9}$-GFP-kan* | This work |
| YSM2046 | *h90 map3::ura4+ Pmap3-map3$^{dn9}$-GFP-kan scd2-mcherry-nat* | This work |
| YSM2047 | *h90 sec6-GFP-ura4+ scd2-mcherry-natMX* | This work |
| YSM2048 | *h90 bgs4::ura4+Pbgs4-GFP-bgs4-leu1+ scd2-mcherry-natMX* | This work |
| YSM2049 | *h90 scd1-3GFP-hph rgs1::kanMX* | This work |
| YSM2050 | *h90 scd2-mCherry-natMX ura4-294::Pshk1-ScGIC2-CRIB-3GFP-ura4+* | This work |
| YSM2122 | *h90 ura4-294::Pshk1-ScGIC2-CRIB-3GFP-ura4+* | This work |
| YSM2123 | *h90 bgs1::ura4+Pbgs1-GFP-bgs1-leu1+ scd2-mcherry-natMX* | This work |
| YSM2124 | *h- sxa2::kanMX scd1-3GFP-kanMX pka1::hphMX* | This work |
| YSM2125 | *h90 map3::ura4+ Pmap3-map3-GFP-kan* | This work |
| YSM2126 | *h90 map3::ura4+ Pmap3-map3-GFP-kan rgs1::hphMX* | This work |

## Supplemental Experimental Procedures

### Strains, Media, and Growth Conditions

*S. pombe* strains used are listed in Supplementary Table 1. Cells were grown in MSL +N or MSL –N (minimal sporulation liquid or agar) [33]. MSL –N solid media was used as either 2% agar plates or 2% electrophoresis-grade agarose pads. Agarose pads were covered with a coverslip and sealed with VALAP (1:1:1 Vaseline:Lanolin:Paraffin). Strains containing *sxa2::kanMX* and *rgs1::kanMX* mutations were obtained from the Bioneer haploid mutant collection and verified by diagnostic PCR. For construction of *scd2-mCherry-natMX6*, a PCR-based approach was used with plasmid pFA6a-*mCherry-NatMX6 [34]* and oligos with homology to 78 nt directly upstream and 78 nt downstream the stop codon. Gene disruptions and tagging were confirmed by diagnostic PCR for both sides of the gene replacements or insertions. P-factor pheromone was purchased from Pepnome (Zhuhai City, China) and used from a stock solution of 1 mg/ml in methanol. CellMask orange plasma membrane strain (C10045) was purchased from Invitrogen and added to mating cells at a final concentration of 2 µg/ml for 10 minutes followed by a single wash with MSL-N before imaging.

### Mating Assays

Cells were grown in pre-culture in MSL +N at 25ºC to $OD_{600}$=0.4 to 1 and diluted to $OD_{600}$=0.025 in MSL +N (for heterothallic mixtures in Fig. S1F cells were mixed in equal parts). Cells were then grown for 18-24 hours to $OD_{600}$=0.4 to 1 at either 25 or 30ºC in MSL+N. Cells were harvested by centrifugation and washed 3 times in MSL –N. From here, cells were treated in one of three different ways depending on the experiment. For most fluorescent imaging (Fig. 1D-G, Fig. 2A-D, Fig. 3C-D and Fig. S1B-E, Fig. S2A-E), cells were placed onto MSL –N plates and incubated for 18 hours at 18$^{o}$C. Cells were then resuspended in MSL –N liquid and placed onto MSL –N pad for imaging. For DIC imaging of pre-arrested cells or CRIB-GFP imaging (Fig.1A-C, Fig. 3E-F and Fig.S1A), cells were resuspended to $OD_{600}$=20 and 0.3 µl placed onto MSL –N pads. For heterothallic cells in Fig. S1F, cells were resuspended to $OD_{600}$=1.5 and allowed to arrest in G1 at 30$^{o}$C for 4 hours and placed onto MSL –N pad.
We note that CRIB-GFP expression did not seem to have an effect on mating properties: *h90* CRIB-GFP cells mated with similar kinetics and efficiency as wildtype cells. We further note that Scd2 dynamics observed in CRIB-GFP-expressing cells was indistinguishable from that of wildtype cells.

### Pheromone Treatment

Heterothallic cells were grown in pre-culture in MSL +N at 25$^{o}$C to $OD_{600}$=0.4 to 1 and diluted to $OD_{600}$=0.025 in MSL +N. Cells were then grown for 18 hours to $OD_{600}$=0.4 to 1 at 30$^{o}$C. Cells were washed 3 times in MSL –N and resuspended to $OD_{600}$=1.5 and allowed to arrest in G1 at 30$^{o}$C for 4 hours and placed onto MSL –N pad (Fig. 3A) or 35mm petri plate (Fig. 3B) with methanol or P-factor. For cells treated with additional P-factor, 2 µl of P-factor (or methanol as control) was added around all four sides of cover slip and incubated for an additional 18 hours. For imaging of Scd1-3GFP in *pka1*Δ (Fig. S3B*)*, cells were grown in MSL+N at 25 $^{o}$C to $OD_{600}$=0.6-0.8 and placed directly onto MSL+N pads with methanol or P-factor and incubated 14 hours at 18 $^{o}$C before imaging.

**Microscopy and Image Analysis**

Images were acquired on either a spinning disk confocal microscope or a DeltaVision epifluorescence system. The DeltaVision platform (Applied Precision) was composed of a customized Olympus IX-71 inverted microscope and a Plan Apo 60×/1.42 NA (for DIC) or a U-Plan Apo 100×/1.4 NA oil objective (for fluorescence), a CoolSNAP HQ2 camera (Photometrics), and an Insight SSI 7 color combined unit illuminator. To limit photobleaching, images in Fig. 1D, F-G, Fig. 3A, and Fig. S1C-D, Fig. S1F and Fig. S2A were captured by OAI (optical axis integration) imaging of a 4.6 μm z section, which is essentially a real time z sweep. High-resolution imaging was performed with either the Delta Vision or spinning disk confocal microscope. For Delta Vision imaging, optical z slices were captured every 0.3 μm (Fig. S1E) or every 0.6 μm (Fig. 3B-D) and maximum projections are shown. Images were acquired with softWoRx software. The spinning disk microscope system was as previously described [35]. For spinning disk confocal imaging (Fig. 1C and E, Fig. 2A-D, Fig. S2B-E and Fig. S3B) optical slices were acquired every 0.6 μm and maximum projections are shown for all except for Fig. S2B and E and the right panels of C where the medial optical slice is shown. Control experiments confirmed co-localization was not the result of optical bleed-through between the green and red channels by imaging single color fluorescent strains. All imaging was performed at room temperature (20-22$^{o}$C).

Peripheral kymographs were constructed in ImageJ v1.46 by drawing a 5 pixel (0.65 μm) line around the cell cortex. Zone properties (Fig. 1G) were calculated from 20 kymographs by placing oval ROIs over areas visually deemed a zone. Quantification of shmoo position (Figure 1B, upper) was accomplished by determining the origin of each shmoo. Tip shmoos were those that originated from within the hemispherical cell tip and side shmoos if originated between the two hemispherical cell tips. Shmoo angles (Figure 1B, lower) were measured with the ObjectJ plugin for Image J by comparing the axis of shmoo growth to the axis of growth before arrest with 0$^{o}$ indicating no change in direction and 90$^{o}$ representing shmoo growth perpendicular to the growth axis before arrest. We note that for this analysis the cellular location of the shmoo is not included and could have originated from the cell tip or cell side. The distribution of shmoo angles in Fig. 1B and Fig. 3E are shown graphically by binning the angles into 15$^{o}$ groups from 0 to 90$^{o}$. The length of the pie slice represents the percent of angles in each angle group normalized to the maximum.

Figures were assembled with Adobe Photoshop CS5 and Adobe Illustrator CS5.

**Calculation of Engagement Frequencies**

Mating behavior frequencies were calculated as follows, with fused pairs (asci) and tetrads counting as two cells: Engagement frequency = (engaged cells)/((engaged cells) + (non-engaged shmooing cells) + (unmated cells)). Non-engaged shmooing cell frequency = (non-engaged shmooing cells)/((engaged cells) + (non-engaged shmooing cells) + (unmated cells)). 3 partners group frequency = (engaged triplets)/(engaged cells). Sister pair frequency = (engaged sisters)/(engaged cells).

**Determination of Mating-Type Switching Rates and Partner Choice of Compatible Sister Cells**

The rate of mating type switching in wt *h90 map3-GFP*, *h90 map3$^{dn9}$-GFP and h90 rgs1*Δ *map3-GFP* strains was calculated by determining the percent of compatible sister pairs (one *h*+ and one *h*-) amongst all sister pairs. This was done by timelapse imaging of Map3($^{dn9}$)-GFP

expression during growth arrest and the subsequent mating response on MSL-N agarose pads. As the Map3 M-factor receptor is only expressed in *h*+ cells , compatible sisters cells were determined as sister pairs where only one cell showed a GFP signal.

For determining the partner choice of compatible sisters, the percent of sisters that chose another cell over a compatible sister was assessed. Sister pairs were included in the analysis only if of opposite mating types (as assessed from Map3-GFP expression) and in close proximity of at least one other compatible cell. Only the choice of the first sister cell to mate was considered, as the second cell to engage no longer has an available sister.

**Estimation of Cell Volume And Cell Surfaces**

Cell dimensions were measured from DIC images using the ObjectJ plugin for ImageJ. The volume of rod shaped and shmooing cells were calculated as a cylinder with two hemispherical caps where *r* is the radius and h is the height of a cylinder (total length - 2*r*): $(4/3)\pi r^3 + \pi r^3 h$. The surface of each hemispherical end is $(4\pi r^2)/2$ and the surface of the cylinder is $2\pi rh$. As starved, exploring cells are about 6 μm in length and 4 μm wide, cell side surface represents about 33% of the total surface.

**Supplemental References**


33. Egel, R., Willer, M., Kjaerulff, S., Davey, J., and Nielsen, O. (1994). Assessment of pheromone production and response in fission yeast by a halo test of induced sporulation. Yeast *10*, 1347-1354.
34. Snaith, H.A., Samejima, I., and Sawin, K.E. (2005). Multistep and multimode cortical anchoring of tea1p at cell tips in fission yeast. Embo J *24*, 3690-3699.
35. Bendezú, F.O., Vincenzetti, V., and Martin, S.G. (2012). Fission yeast sec3 and exo70 are transported on actin cables and localize the exocyst complex to cell poles. PLoS One *7*, e40248.